

Received December 8, 2018, accepted December 18, 2018, date of publication December 24, 2018, date of current version January 11, 2019.

Digital Object Identifier 10.1109/ACCESS.2018.2889370

Full State Tracking and Formation Control for Under-Actuated VTOL UAVs

XIUHUI PENG¹, KEXIN GUO^{2,3}, AND ZHIYONG GENG¹

¹State Key Laboratory for Turbulence and Complex Systems, Department of Mechanics and Engineering Science, College of Engineering, Peking University, Beijing 100871, China

²School of Electrical and Electronic Engineering, Nanyang Technological University, Singapore 639798

³Hangzhou Innovation Institute of Beihang University, Hangzhou 310051, China

Corresponding author: Zhiyong Geng (zygeng@pku.edu.cn)

This work was supported by the National Natural Science Foundation of China under Grant 61773024.

ABSTRACT In this paper, a coupled-attitude based trajectory tracking scheme is proposed to track both the position and attitude of under-actuated unmanned aerial vehicles, and its application on formation control is further demonstrated. An intermediate attitude which is composed of the desired attitude and position information is designed in a two-stage framework, wherein the first stage is the controller design of a translational subsystem and the second stage is that of an attitude subsystem. By virtue of the intermediate attitude, trajectory tracking which includes both attitude and position is realized. The proposed intermediate attitude can be viewed as a bridge connecting the position and attitude motion, and it is a new approach for both single and multiple under-actuated rigid bodies' control. Based on the approach of coupled-attitude-based trajectory tracking, both the set point stabilization and formation tracking tasks for under-actuated vertical takeoff and landing vehicles over a directed acyclic graph can be achieved. The performances of the proposed control laws are illustrated through numerical simulations.

INDEX TERMS Intermediate attitude, coupled-attitude based scheme, under-actuated VTOL UAVs, formation tracking.

I. INTRODUCTION

Formation control of multi-agent systems has attracted enormous research efforts during the past decades. Motivation for such research stems from the inherent strength and robustness of a coordinated group when dealing with tasks such as searching, surveying, mapping, surveillance and rescue missions [1]–[5]. From the vantage point of networked control, formation control is a cooperative control with its nodes being vehicles subject to some given communication topologies [2]. The dynamics of the networked system depend not only on the dynamics of the nodes but also on the communication topology.

Multi-agent system control is originated from the study of the dynamics of multiple integrators in [6] and [7], which mainly focusing on the communication topology between agents and the coordinated behaviors of the group. The results on networked integrators are rich and diverse. The dynamics of integrators can be treated as the dynamics of points mass, which is reasonable when the vehicles are far from each other. Taking into account the dynamic model of the nodes, [8]–[10] investigated the consensus and formation control

for multiple linear systems by locally approximating the model of the vehicle as a rigid body through linearization near some equilibrium. Nevertheless, compared with integrators, a real-world system has more complex dynamical behaviors.

For the problem of coordination undergoing a large range of motion, especially when the initial state of vehicles are far from the coordinated state, the nonlinearity cannot be neglected. Some researchers considered the Euler-Lagrange (EL) systems as the dynamics of the nodes in the network, and made a significant progress in the study of consensus and cooperative control [11], [12]. Properly speaking, the global position and attitude of a vehicle are described by a Special Euclidean group $SE(3)/SE(2)$, which is a nonlinear manifold. However, the EL systems are modeled on the Euclidean space by local parameterization on the manifold. Since, in practice, the maneuverable vehicles require larger ranges of motion, it will be more meaningful if the dynamics of vehicles is described on nonlinear manifold directly.

Inspired by the multi-agent control in [2], [6], [8], and [11], the cooperative control of multiple vehicles on the

nonlinear manifold was studied [13], and some notable results have been released in [14]–[19]. In [15], for the vehicles that rotate freely in the three-dimensional (3D) space, such as satellites, the attitude synchronization on the Special Orthogonal group $SO(3)$, which is also a nonlinear manifold, was studied. The pose (which contains both the position and attitude) synchronization and formation problems were investigated in [16] and [18], and the cooperative control of multiple vehicles on $SE(3)$ with finite time convergent rate was considered in [19]. Note that those vehicles are fully-actuated. In practice, most vehicles exhibit the non-holonomic constraints or under-actuated properties, such as non-holonomic unicycle-type vehicles in 2D space and under-actuated quadrotor aircraft in 3D space [13], [20], [21].

The under-actuated vehicles are those having their degrees-of-freedom larger than the number of the corresponding control inputs. In some cases, the linearization systems of under-actuated vehicles is noncontrollable [22]. Hence, it is an inevitable trend to study multiple vehicles on nonlinear manifolds. This paper studies the formation tracking control for a class of under-actuated vertical take-off and landing (VTOL) unmanned aerial vehicles (UAVs) with dynamics evolving on a nonlinear manifold. Since the trajectory tracking problem is a prerequisite for the formation tracking task, thus, in this paper we first study the trajectory tracking problem of under-actuated VTOL UAVs.

We note that the position control for under-actuated VTOL vehicles has been studied in [23]–[31]. In those literatures, a general framework, which decomposes the overall system into an outer translational control loop and an inner attitude control loop, was proposed for position tracking. Based on the unit quaternion which can represent the attitude, a position controller without linear velocity measurements was constructed in [23], and [24] designed an adaptive position controller for a perturbed rigid body. The rotation matrix-based controller was designed in [26] with almost-global stabilization, and a global controller through a hybrid control strategy was proposed in [27]. The objective of the above research is to track a desired position trajectory which is specified a priori, wherein the desired rotation attitude matrix constructed by position error aims to assist in the controller to achieve the position tracking, and this matrix can be regarded as an auxiliary desired attitude. In practice, the desired trajectory is actually generated by a real under-actuated VTOL UAV which includes both the position and attitude rather than an arbitrary position trajectory. For example, a group of quadcopters solidly equipped with some sensors aim to inspect the surface of a huge object or construct a whole map of an unknown environment in a cooperative way. Fig. 1 illustrates four VTOL UAVs performing formation flying in 3D space where the headmost UAV is viewed as the leader to be tracked by the other three followers. Other applications, such as environment surveillance, search and rescue, also require the coordination of both the position and attitude. Here, the control challenge is to simultaneously track both the desired position and attitude. To tackle this



FIGURE 1. Leader-follower formation tracking of four under-actuated VTOL UAVs. They are cooperatively conducting a surface inspection task. The dark UAV serves as the leader and the others are the followers.

problem, this paper proposes a coupled-attitude based trajectory tracking approach. In addition, relying on the coupled-attitude trajectory tracking approach and geometric convexity on the nonlinear manifold, a formation tracking is studied with respect to a directed acyclic graph. The directed acyclic graph is widely used in the cooperative control of networked systems. For example, the vehicle is able to observe the position of its parent nodes using the onboard forward sensing sensors [33]. In contrast to a directed tree graph in which each follower has and only has one parent node, for a directed acyclic graph, each follower may obtain information from more than one parent nodes. This property helps the directed acyclic graph increase the robustness of communication so that the networked systems could perform the cooperative task even if one parent node is broken. The main contributions of this paper are as follows:

1. A coupled-attitude based trajectory tracking scheme is proposed. An intermediary attitude is presented for under-actuated VTOL UAV to realize the full state tracking. This intermediate attitude is first proposed in this paper. Coupling the position and attitude information of the under-actuated VTOL UAVs, the proposed intermediary attitude is able to control the under-actuated VTOL UAVs so that the position and attitude of both a static and mobile VTOL UAV can be tracked.
2. Based on the proposed coupled-attitude based trajectory tracking approach, a formation tracking strategy of multiple VTOL UAVs is demonstrated by constructing a virtual leader through a directed acyclic graph, which is more general than a directed tree. Besides, the set point stabilization of multiple UAVs is feasible for landing and hovering.

The remainder of this paper is structured as follows. Some mathematical preliminaries and the problem formulation are introduced in Section II. The coupled-attitude based trajectory tracking scheme and trajectory tracking controller design are presented in Section III. Section IV introduces a formation tracking control law. Simulations are conducted in Section V. Finally, conclusions are drawn in Section VI.

II. PROBLEM FORMULATION

A. SYSTEM MODEL

In this paper, based on the Newton-Euler equations, the underactuated VTOL UAV can be modeled as

$$\begin{cases} \dot{p} = v, \\ \dot{v} = ge_3 - (f/m)Re_3, \end{cases} \quad (1a)$$

$$\begin{cases} \dot{R} = R\hat{\omega}, \\ J\dot{\omega} = (J\omega)^\wedge\omega + \tau, \end{cases} \quad (1b)$$

where $p, v \in \mathbb{R}^3$ are the position and linear velocity in the inertial frame \mathcal{F}_I , $R \in SO(3) := \{R \in \mathbb{R}^{3 \times 3} | R^T R = RR^T = I_3, \det(R) = 1\}$ denotes the rotation matrix from the body-fixed frame \mathcal{F}_B to the inertial frame \mathcal{F}_I , $\omega \in \mathbb{R}^3$ is the angular velocity in \mathcal{F}_B , $g \in \mathbb{R}$ is the gravitational acceleration, $e_3 = [0, 0, 1]^T$, $m \in \mathbb{R}^+$ and $J \in \mathbb{R}^{3 \times 3}$ are the mass and inertia matrix respectively, $f \in \mathbb{R}$ and $\tau \in \mathbb{R}^3$ are the thrust force and control torque. The hat operator $(\cdot)^\wedge : \mathbb{R}^3 \rightarrow \mathfrak{so}(3)$ is the transformation of a vector $x \in \mathbb{R}^3$ to a skew-symmetric matrix $\hat{x} \in \mathfrak{so}(3)$ such that $\hat{x}y = x \times y, \forall x, y \in \mathbb{R}^3$, where $\mathfrak{so}(3) := \{\hat{x} \in \mathbb{R}^{3 \times 3} | \hat{x}^T = -\hat{x}\}$. For example, for any vector $x = [x_1, x_2, x_3]^T \in \mathbb{R}^3$, it follows that

$$\hat{x} = \begin{bmatrix} 0 & -x_3 & x_2 \\ x_3 & 0 & -x_1 \\ -x_2 & x_1 & 0 \end{bmatrix}.$$

The inverse operator that corresponds to the hat $(\cdot)^\wedge$ is the vee operator $(\cdot)^\vee : \mathfrak{so}(3) \rightarrow \mathbb{R}^3$.

The thrust force f and torque τ are generated by an actuation mechanism. For example, a type of these UAVs is the quadrotor where each rotor produces a thrust force f_i which is parallel to the third axis of the UAV. The thrusts $f_i (i = 1, 2, 3, 4)$ are generated by $f_i = c_\omega \varpi_i^2$, where ϖ_i is the i -th rotor's rotational velocity and c_ω is a positive constant. Then, the thrust force f and torque τ are given by $f = f_1 + f_2 + f_3 + f_4$, $\tau_1 = d(f_2 - f_4)$, $\tau_2 = d(f_1 - f_3)$, $\tau_3 = c_\tau(f_1 - f_2 + f_3 - f_4)$, where d is the distance from the vehicle rotor to the mass center, and c_τ denotes the force-to-moment scaling factor.

Notation: Throughout this paper, $\|x\|$ denotes the Euclidean norm of a vector x . Let I_p denote the identity matrix of dimension $p \times p$. $x \in \mathbb{S}^2$ implies $x \in \mathbb{R}^3$ with unit Euclidean norm. $\mathbf{0} \in \mathbb{R}^3$ represents a zero vector. For a matrix X , $\text{tr}(X)$ denotes the trace of the matrix X . Let e_1, e_2, e_3 denote the natural basis of \mathbb{R}^3 . $\text{diag}(x_i)$ represents a block-diagonal matrix with $x_i, i = 1, \dots, n$ on the diagonal.

B. PROBLEM FORMULATION

Consider a group of leader-following UAVs performing a task. Without loss of generality, as shown in Fig. 1, the head-most vehicle can be seen as the leader in a distributed UAV network. The desired trajectory is generated by the

following dynamics of the leader

$$\begin{cases} \dot{p}_d = v_d, \\ \dot{v}_d = ge_3 - (f_d/m)R_d e_3, \end{cases} \quad (2a)$$

$$\begin{cases} \dot{R}_d = R_d \hat{\omega}_d, \\ J \dot{\omega}_d = (J \omega_d)^\wedge \omega_d + \tau_d, \end{cases} \quad (2b)$$

where the subscript d represents the state of the leader. The desired trajectory (2) should satisfy the following assumption.

Assumption 1: The desired thrust force f_d is positive and bounded. In addition, there exists a known constant f_{\min} such that $f_d > f_{\min}$ for all time.

Remark 1: This assumption is not restrictive. Due to the gravity action, the desired attitude needs to satisfy $R_d e_3 = e_3$ and there must exist a positive constant thrust force f_d to offset the gravity action if an under-actuated VTOL UAV stays stationary in the air. Meanwhile, the UAV has upward and downward motions due to the force of gravity and the coordination of the attitude. Thus, even though the thrust force satisfies Assumption 1, the desired trajectory (2) can be arbitrary in 3D space including hovering at some point and also flying in the air.

The main objective in our work is to propose a approach to track the reference state generated by the leader system (2). Inspired by the related works [23], [24], [26], [27], [29], a coupled-attitude based trajectory tracking scheme is proposed in this paper. We introduce an intermediate attitude which can be viewed as a bridge connecting the position and attitude motion. Based on the proposed scheme, the translational and rotational controllers are designed stage by stage for the under-actuated VTOL UAVs (1) to achieve the set point stabilization, trajectory tracking and also formation tracking.

III. COUPLED-ATTITUDE BASED TRAJECTORY TRACKING DESIGN

In this section, we first introduce a coupled-attitude based trajectory tracking scheme. Then, based on this scheme, the controllers, including the position thrust force and attitude torque controllers, are proposed and the corresponding stability is analyzed. Finally, as a special case, the set point stabilization problem is discussed.

To design a trajectory tracking control law, the translational dynamics of under-actuated VTOL UAV in (1a) can be rewritten as

$$\begin{cases} \dot{p} = v, \\ \dot{v} = ge_3 - F + \Delta, \end{cases} \quad (3)$$

where $F = (f/m)R_c e_3 \in \mathbb{R}^3$ is a virtual control variable, $R_c \in SO(3)$ is a useful intermediary smooth rotation matrix to achieve trajectory tracking, $\Delta = (f/m)(R_c - R)e_3 \in \mathbb{R}^3$ is a perturbed term. Next, we introduce the proposed coupled-attitude based trajectory tracking scheme for the full state control of the under-actuated VTOL UAV, and then the

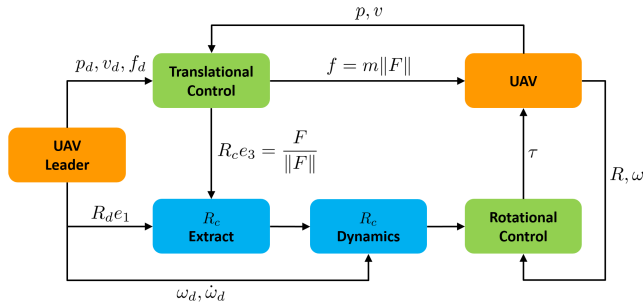


FIGURE 2. The novel two-stage trajectory tracking framework for under-actuated VTOL UAVs.

trajectory tracking controller and set point stabilization controller are presented, respectively.

A. COUPLED-ATTITUDE CONTROL SCHEME

Let $e_p = p - p_d$ and $e_v = v - v_d$ be the position and linear velocity tracking errors, respectively. Let $E = R_c^T R$ be the orientation error between the orientation of the rigid body and the orientation of the intermediary smooth rotation matrix R_c . Then, the dynamics of the error systems can be written as follows.

$$\begin{cases} \dot{e}_p = e_v, \\ \dot{e}_v = (f_d/m)R_d e_3 - F + \Delta, \end{cases} \quad (4a)$$

$$\begin{cases} \dot{E} = E \hat{e}_\omega, \\ J \dot{e}_\omega = (J\omega)^\wedge \omega + J \hat{e}_\omega E^T \omega_c - J E^T \dot{\omega}_c + \tau, \end{cases} \quad (4b)$$

where $e_\omega = \omega - E^T \omega_c \in \mathbb{R}^3$ is the angular tracking error, ω_c and $\dot{\omega}_c$ are determined by the rotation matrix R_c and its derivative.

Definition 1: In the full state tracking problem of under-actuated VTOL UAVs, the rotation matrix R_c is named as the intermediary attitude.

Note that from the expression, the attitude subsystem (1b) is not influenced by the translational subsystem (1a), however, the evolution of the position is indeed controlled by the attitude since the change of the linear velocity results from the change of the attitude. The proposed coupled-attitude based trajectory tracking scheme is shown in Fig. 2. Note that (4a) is a second order system with a perturbation, and the designed translational input F , which will be introduced in (11), contains both the position and the desired attitude information. Meanwhile, the translational control F will be feedback to construct the intermediary smooth rotation matrix R_c . The novelty of intermediate attitude is that R_c in (5)-(7) is constructed from both the translational control input F and the desired attitude vector $R_d e_1$ which is not parallel to $R_c e_3$. The aim is to let the actual attitude R track the intermediary attitude R_c . Furthermore, the attitude controller relies on both the position and the desired attitude since R_c is applied in the attitude control torque design. Once the position error converges to zero, the intermediate rotation matrix R_c will be consistent with the desired rotation

matrix R_d . Thus, the actual attitude will converge to the desired attitude as well. Next, we will introduce the construction of R_c .

Suppose that the virtual control input F can be written as $F = y(e_p, e_v, f_d, R_d)$ and $\|F\| \neq 0$, where $y(\cdot)$ is a function, then the third column vector of the intermediary smooth rotation matrix R_c can be constructed as

$$b_{3c} = \frac{F}{\|F\|}, \quad (5)$$

where $b_{3c} := R_c e_3$. Denote $b_{1d} = R_d e_1$. Suppose the vector b_{1d} is not parallel to b_{3c} , then the other two column vectors of R_c can be constructed as

$$b_{2c} = \frac{b_{3c} \times b_{1d}}{\|b_{3c} \times b_{1d}\|}, \quad b_{1c} = b_{2c} \times b_{3c}, \quad (6)$$

Thus, the intermediary attitude R_c can be given by

$$R_c = [b_{1c}, b_{2c}, b_{3c}] \in SO(3). \quad (7)$$

The dynamics of rotation matrix R_c has the form of $\dot{R}_c = R_c \hat{\omega}_c$. Thus, the angular velocity ω_c and angular acceleration $\dot{\omega}_c$ can be obtained through $\omega_c = (R_c^T \dot{R}_c)^\vee$ and $\dot{\omega}_c = (-\hat{\omega}_c R_c^T \dot{R}_c + R_c^T \ddot{R}_c)^\vee$.

Remark 2: The rotation matrix R_c is named as the intermediary attitude since it will evolve into the desired rotation matrix R_d with $b_{3c} \rightarrow b_{3d}$ when $e_p \rightarrow 0$, $e_v \rightarrow 0$, where $b_{3d} = R_d e_3$. The objective of some related results [23], [24], [26], [27], [29] is to design an appropriate control force f and torque τ for the under-actuated VTOL UAVs to track a smooth desired trajectory p_d without considering the desired attitude R_d . As an auxiliary value, a desired attitude is also constructed in these papers. However, this desired attitude just assists the vehicle to track the desired position. Thus, the rotation matrix constructed in these papers can be named as an auxiliary attitude.

To proceed, the following lemma is introduced first.

Lemma 1: If the vector $b_{3c} = b_{3d}$, then, the intermediary rotation matrix R_c will be consistent with the desired rotation matrix R_d .

Proof: Let ϕ_d, θ_d, ψ_d denote the roll, pitch, yaw angle in the Euler angles. Then, the desired rotation matrix R_d can be rewritten as (8). Based on the expression (8) and its calculation, we can obtain $b_{1c} = b_{1d}$ and $b_{2c} = b_{2d}$ in equation (6) if $b_{3c} = b_{3d}$. Thus, the fact that $R_c = R_d$ when $b_{3c} = b_{3d}$ is proved. \square

Remark 3: In this paper, the under-actuated VTOL UAVs have four control inputs but six degree-of-freedom. For other under-actuated vehicles whose number of degree-of-freedom is larger than the control inputs, the proposed idea of the intermediary attitude also works. In 3D space, the intermediary attitude can be applied to the tracking control of the vehicle which has three control inputs but six degree-of-freedom, such as the unmanned fixed-wing aircraft. In such case, one input aims to control the position and others control the attitude. The proposed coupled-attitude based trajectory tracking scheme, which couples the position and attitude

$$R_d = \begin{bmatrix} \cos(\psi_d) \cos(\theta_d) & -\sin(\psi_d) \cos(\phi_d) + \sin(\phi_d) \sin(\theta_d) \cos(\psi_d) & \sin(\psi_d) \sin(\phi_d) + \sin(\theta_d) \cos(\psi_d) \cos(\phi_d) \\ \sin(\psi_d) \cos(\theta_d) & \cos(\psi_d) \cos(\phi_d) + \sin(\phi_d) \sin(\theta_d) \sin(\psi_d) & -\cos(\psi_d) \sin(\phi_d) + \sin(\theta_d) \sin(\psi_d) \cos(\phi_d) \\ -\sin(\theta_d) & \sin(\phi_d) \cos(\theta_d) & \cos(\phi_d) \cos(\theta_d) \end{bmatrix}. \quad (8)$$

information of these under-actuated vehicles, is still feasible to solve the control problems of these vehicles such as set point stabilization, tracking and formation.

B. CONTROLLER DESIGN AND STABILITY ANALYSIS

Before proceeding, suppose that the perturbed term Δ is zero, and the following error dynamics is obtained

$$\begin{cases} \dot{e}_p = e_v, \\ \dot{e}_v = (f_d/m)R_d e_3 - F, \end{cases} \quad (9)$$

Based on the Rodrigues' formula [13], the rotation error matrix $E \in SO(3)$ can be expressed by the unique rotational axis $n_e \in \mathbb{S}^2$ and angle $|\theta_e| < \pi$, such that

$$E = \exp(\hat{n}_e \theta_e) = I_3 + \sin(\theta_e) \hat{n}_e + (1 - \cos(\theta_e)) \hat{n}_e^2. \quad (10)$$

Inspired by the stability results of [27], [29], and [32], the following useful lemma is presented firstly.

Lemma 2 [27], [29], [32]: *Suppose there exist a thrust force f and a torque τ that can stabilize the state of the systems (9) and (4b) asymptotically, and there exists a positive constant φ such that $\|\Delta\| < \varphi\|\theta_e\|$, then the error systems (4a) and (4b) are asymptotically stable.*

By virtue of Lemma 2, the trajectory tracking problem becomes stabilizing the error dynamic systems with a bounded term such that $\|\Delta\| < \varphi\|\theta_e\|$. Here, the hierarchical controller, which contains a position subcontroller and an attitude subcontroller, is adopted in this paper. Next, we will design the control force f and torque τ to stabilize the position error system (9) and attitude error system (4b) respectively, which guarantees the boundedness of the perturbed term Δ as well.

1) POSITION THRUST FORCE DESIGN

Since the boundedness of the perturbed term Δ is required for the overall system, the thrust force f should be boundedness as well. Thus, to guarantee its boundedness, the virtual control input is proposed as follows

$$F = k_1 \frac{e_p}{\sqrt{1 + e_p^T e_p}} + k_2 \frac{e_v}{\sqrt{1 + e_v^T e_v}} + \frac{f_d}{m} R_d e_3, \quad (11)$$

where $k_1, k_2 > 0$ are positive constants satisfying $f_{min} - m(k_1 + k_2) > 0$. Since $F = (f/m)R_d e_3$ and $b_{3c} := R_d e_3 = F/\|F\|$, the thrust force f can be given by

$$f = m\|F\|. \quad (12)$$

The following lemma provides the stability of the translational control loop in the absence of the perturbed term.

Lemma 3: *Considering the position error system (9) satisfying Assumption 1, under the virtual control input given by (11), the position system (9) is asymptotically stable.*

Proof: Substituting (11) into (9), it yields

$$\dot{e}_v = -k_1 \frac{e_p}{\sqrt{1 + e_p^T e_p}} - k_2 \frac{e_v}{\sqrt{1 + e_v^T e_v}}. \quad (13)$$

Then, a Lyapunov function is defined as follows

$$V_p = k_1(\sqrt{1 + e_p^T e_p} - 1) + \frac{1}{2} e_v^T e_v, \quad (14)$$

and its time derivative is given by

$$\begin{aligned} \dot{V}_p &= k_1 \frac{e_p^T \dot{e}_p}{\sqrt{1 + e_p^T e_p}} + e_v^T \dot{e}_v \\ &= -k_2 \frac{e_v^T e_v}{\sqrt{1 + e_v^T e_v}} \leq 0, \end{aligned} \quad (15)$$

which implies that the position error system (9) is Lyapunov stable. Furthermore, the function V_p is nonincreasing, which hints that $\lim_{t \rightarrow \infty} \int_0^t \dot{V}_p(\tau) d\tau$ exists and is finite. Since $V_p(t) \leq V_p(0)$, then, $e_p(t)$ and $e_v(t)$ are always bounded. Note that e_v is uniformly continuous with respect to t since \dot{e}_v is bounded. Thus, \dot{V}_p is uniformly continuous. Based on Barbalat's Lemma, it follows that $\dot{V}_p \rightarrow 0$, i.e., $e_v \rightarrow 0$ as $t \rightarrow \infty$. Then, from equation (13), one has $e_p \rightarrow 0$ as $t \rightarrow \infty$ and V_p is radially bounded. Hence, the position error system (9) is asymptotically stable. \square

2) ATTITUDE TORQUE DESIGN

Suppose the rotation matrix R_c generated from F and R_d is smooth, then the attitude torque τ of (4b) can be designed as

$$\tau = -\alpha_1 e_E - \alpha_2 e_\omega - (J\omega)^\wedge \omega - J \hat{e}_\omega E^T \omega_c + J E^T \dot{\omega}_c, \quad (16)$$

where α_1, α_2 are positive definite constants, and the attitude error e_E is given by

$$e_E = \frac{1}{2(1 + \text{tr}(E))} (E - E^T)^\vee. \quad (17)$$

Thus, the following lemma gives the stability of the attitude control loop.

Lemma 4: *Consider a smooth R_c which is obtained from F and R_d , and the initial rotation matrix E which is in the set $D = \{E \in SO(3) | \text{tr}(E) > -1\}$. Driven by the control torque (16), the attitude error system (4b) is almost globally asymptotically stable.*

Proof: Substituting torque (16) into the second equation (4b), it obtains

$$J \dot{e}_\omega = -\alpha_1 e_E - \alpha_2 e_\omega. \quad (18)$$

Let us consider the following positive definite Lyapunov function

$$V_R = \alpha_1 \Psi + \frac{1}{2} e_\omega^T J e_\omega, \quad (19)$$

where the attitude error function is defined as $\Psi = \ln(2) - \frac{1}{2} \ln(1 + \text{tr}(E))$ [34]. The attitude error function Ψ is well defined in the set D . Then, the time derivative of V_R is given as

$$\begin{aligned} \dot{V}_R &= \alpha_1 e_E^T e_\omega + e_\omega^T J \dot{e}_\omega \\ &= -\alpha_2 e_\omega^T e_\omega, \end{aligned} \quad (20)$$

which implies that the attitude error system (4b) is Lyapunov stable. In addition, the function V_R is nonincreasing, which hints that $\lim_{t \rightarrow \infty} \int_0^t \dot{V}_R(\tau) d\tau$ exists and is finite. Meanwhile, the other three undesired equilibriums (i.e. the undesired set $E = \{\text{diag}(1, -1, -1), \text{diag}(-1, 1, -1), \text{diag}(-1, -1, 1)\}$) are excluded since the function $V_R \rightarrow \infty$ as the state tend to the undesired equilibriums [13]. Since $V_R(t) \leq V_R(0)$, then, $e_E(t)$ and $e_\omega(t)$ are always bounded. Note that e_ω is uniformly continuous with respect to t since \dot{e}_ω is bounded. Hence, \dot{V}_R is uniformly continuous. By virtue of Barbalat's Lemma, it follows that $\dot{V}_R \rightarrow 0$, i.e. $e_\omega \rightarrow 0$ as $t \rightarrow \infty$. Then, from equation (18), one has $E \rightarrow I_3$ as $t \rightarrow \infty$ and V_R is radially bounded. Thus, the attitude error system (4b) is almost globally asymptotically stable. \square

3) STABILITY OF THE OVERALL SYSTEM

Theorem 1: For the tracking error system (4), under the assumption of $b_{1d} \nparallel b_{3c}$, if the thrust force f and the torque τ are given by (12) and (16), then the overall system is asymptotically stable.

Proof: Based on equation (11) and $f_{\min} - m(k_1 + k_2) > 0$, one has

$$\begin{aligned} f &\geq m \left\| \frac{f_d}{m} R_d e_3 \right\| - m \|k_1 \frac{e_p}{\sqrt{1 + e_p^T e_p}} + k_2 \frac{e_v}{\sqrt{1 + e_v^T e_v}}\| \\ &\geq f_d - m(k_1 + k_2) \geq f_{\min} - m(k_1 + k_2) > 0 \end{aligned} \quad (21)$$

Thus, the singularity $\|F\| \neq 0$ is guaranteed. Under the assumption $b_{1d} \nparallel b_{3c}$, one has that the intermediary rotation matrix R_c is smooth. Then, based on Lemma 3 and Lemma 4, one has that the position error system (9) and attitude error system (4b) are asymptotically stable, respectively. The following parts will give the proof of the boundedness of perturbed term Δ and $R_c^T R_d = I_3$ as $t \rightarrow \infty$.

To show the perturbed term is bounded, we need to prove the boundedness of thrust force f and $(R_c - R)e_3$, respectively. From Assumption 1, together with $R_d \in SO(3)$, it leads that

$$f = m\|F\| \leq m(k_1 + k_2) + f_d \leq \eta, \quad (22)$$

where η is a positive constant. This proves the boundness of thrust force. The boundedness term of $(R_c - R)e_3$ can be checked in [29], and it holds that

$$\begin{aligned} \|(R_c - R)e_3\| &= \|(E - I_3)e_3\| \\ &\leq \sqrt{\text{tr}((E - I_3)^T (E - I_3))} \\ &= \sqrt{2\text{tr}(I_3 - E)} \\ &= \sqrt{4(1 - \cos(\theta_e))} \\ &= 2\sqrt{2} \|\sin(\theta_e/2)\|. \end{aligned} \quad (23)$$

Thus, we can obtain that

$$\|\Delta\| \leq \left\| \frac{f}{m} \right\| \|(R_c - R)e_3\| < \varphi \|\theta_e\|, \quad (24)$$

where φ is a bounded positive constant. Based on the conditions of Lemma 2, the asymptotical convergence of the overall error system (4) is achieved.

Since the overall system is asymptotically stable, we can obtain $e_p \rightarrow 0, e_v \rightarrow 0$ as $t \rightarrow \infty$. From (5), we can conclude that $b_{3c} \rightarrow b_{3d}$ as $t \rightarrow \infty$. Finally, based on the result of Lemma 1, $R_c^T R_d = I_3$ holds. \square

Remark 4: Since an under-actuated VTOL UAV only has a thrust force in position subsystem, its position and attitude motion must be coupled. We propose a coupled-attitude based control strategy as seen in Section III-A and an intermediary smooth rotation matrix R_c defined in (5) - (7) in this paper. Note that R_c is globally smooth if b_{1d} is not parallel to b_{3c} . In addition, the map (6) has a singular point in the case where $b_{1d} \parallel b_{3c}$. This case may cause the attitude subsystem unstable, and thus we assume that $b_{1d} \nparallel b_{3c}$ in Theorem 1. Once $b_{1d} \parallel b_{3c}$, the smoothness of the intermediary rotation matrix R_c cannot be guaranteed. To deal with this situation, the approach proposed in [27] is adopted. If $b_{1d} \parallel b_{3c}$ happens, although it is rare in practice, we can choose another $\hat{b}_{1d} \nparallel b_{3c}$ and determine a temporary R_c at this moment. Fortunately, this moment can not last all the time, and by new control input, the position error e_p and linear velocity error e_v will change immediately due to the desired thrust force $f_d > 0$ with $R_d e_3 \neq \mathbf{0}$. Accordingly, the updated e_p and e_v make $b_{1d} \nparallel b_{3c}$ in the next moment. Thus, the conditions that $b_{1d} \nparallel b_{3c}$ are resatisfied, and the overall system is of asymptotic convergence.

C. SET POINT STABILIZATION CONTROLLER DESIGN

In this subsection, the set point stabilization problem will be studied, where both p_d and R_d are constants. The vehicle under these non-holonomic constraints is in fact a kind of under-actuated vehicle. It is well known that the trajectory tracking control law in [35] for the vehicle with non-holonomic constraints can not be applied to the set point stabilization directly, since the persistent excitation conditions are the prerequisites of the tracking control law [36]. In this paper, the under-actuated VTOL UAVs have four inputs and six outputs, thus the static configuration needs to satisfy these under-actuation constraints. From (2a), the desired constant rotation matrix R_d should satisfy $R_d e_3 = e_3$ to counteract the effect of gravity. Since $R_d e_3 = e_3$, it also requires the roll angle (ϕ_d) and pitch angle (θ_d) should be zero, but the yaw angle (ψ_d) can be specified according to the task. Thus, there exists a positive constant thrust force $f_d = (mg e_3)(R_d e_3)^T = mg$. Note that if $R_d e_3 \neq e_3$ (i.e., $\phi_d \neq 0, \theta_d \neq 0$), the under-actuated VTOL UAV can not be stationary at a point.

Fortunately, with a positive constant thrust force f_d , the set point stabilization problem can be converted to the trajectory tracking problem as discussed in the preceding sections. Similarly, let $e_p = p - p_d, e_v = v, E = R_d^T R$, and e_E is the same

as (17). Then, we present the following corollary, and the proof is omitted since it is similar to the proof of Theorem 1.

Corollary 1: Consider the tracking error systems in (4a) and (4b) with p_d and R_d being configured as some constants and $R_d e_3 = e_3$. Driven by the thrust force f from (11) and (12), and the torque τ from (16), the overall system is asymptotically stable when $b_{1d} \nparallel b_{3c}$.

IV. FORMATION TRACKING CONTROL

The formation tracking controllers for multiple under-actuated VTOL UAVs are presented in this section. Considering $n + 1$ UAVs labeled with $i = 0, 1, \dots, n$, the dynamics of the i -th under-actuated VTOL UAV is given by

$$\begin{cases} \dot{p}_i = v_i, \\ \dot{v}_i = g e_3 - (f_i/m) R_i e_3, \end{cases} \quad (25a)$$

$$\begin{cases} \dot{R}_i = R_i \hat{\omega}_i, \\ J \dot{\omega}_i = (J \omega_i)^\wedge \omega_i + \tau_i, \end{cases} \quad (25b)$$

where node 0 represents the leader and others are the followers.

The communication among n vehicles and the leader is described by a graph $\mathcal{G} = \{\mathcal{V}, \mathcal{E}, \mathcal{A}\}$, where $\mathcal{V} \triangleq \{0, 1, \dots, n\}$ represents the node set, $\mathcal{E} \in \mathcal{V} \times \mathcal{V}$ represents the edge set, and $\mathcal{A} = [a_{ij}] \in \mathbb{R}^{(n+1) \times (n+1)}$ is the adjacent matrix. $a_{ij} > 0$ if $(i, j) \in \mathcal{E}$, and $a_{ij} = 0$ otherwise. Assume that there is no self-loop in the graph, i.e., $a_{ii} = 0$. The node 0 denotes the leader and node i ($i = 1, \dots, n$) represents the i -th follower.

A directed tree is a directed graph where every node, except the one called the root which has no parent, has exactly one parent node. In a directed graph, a cycle represents the directed path that starts and ends at the same node. For the tree graph communication without a circle, it is straightforward to apply the controllers proposed in Theorem 1 for the formation tracking task. To expand, in this paper, we consider a more general tree graph, named directed acyclic graph, which satisfies the following assumption.

Assumption 2: A directed acyclic graph \mathcal{G} is a directed graph with no directed circles, and it has a hierarchical structure.

Fig. 3 indicates the hierarchical structure of a directed acyclic graph, where each node excluding the root node (i.e., leader UAV) and the primary nodes ($i = 1, 2, 3$) may have more than one parent nodes. Compared to the directed tree graph in which each follower has and only has one parent node, the directed acyclic graph increases the communication robustness of the networked systems since each follower may have more than one parent nodes. Based on this kind of graph, to achieve the formation tracking task, a virtual leader tracking structure is proposed in this paper. For the i -th follower, its virtual leader to be tracked is constructed by the information of its parent nodes.

By virtue of geometric convexity on $SO(3)$ proposed in [37], the attitude dynamics of UAV i 's virtual leader is

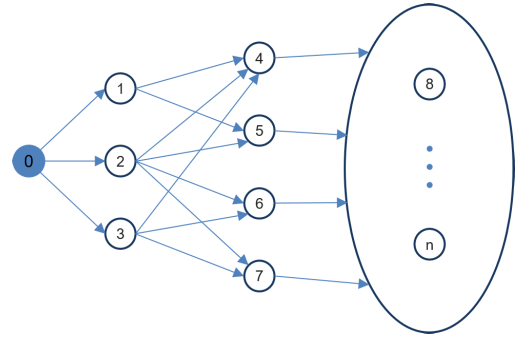


FIGURE 3. The structure of a directed acyclic graph.

constructed as follows

$$\begin{cases} \dot{R}_{vt_i} = R_{vt_i} \hat{\omega}_{vt_i}, \\ J \dot{\omega}_{vt_i} = \sum_{j=0}^n \gamma_{ij} ((J \omega_j)^\wedge \omega_j) + \tau_{vt_i}, \end{cases} \quad (26)$$

where the subscript $vt_i \in \{j | a_{ij} > 0, j = 0, 1, \dots, n\}$, and R_{vt_i} is iteratively defined by

$$\begin{cases} R_{vt_i} = \exp(\lambda_{i0} \log(R_0)), \\ R_{vt_i} = R_{vt_i} \exp(\lambda_{ij} \log(R_{vt_i}^T R_j)), \quad j = 1, \dots, n \end{cases} \quad (27)$$

with the parameter λ_{ij} defined by

$$\lambda_{ij} = \begin{cases} \lambda_{ij} = 0, & a_{ij} = 0 \\ \lambda_{ij} = 1, & j \in \{\min(j) | a_{ij} > 0\} \\ 0 < \lambda_{ij} < 1, & j \notin \{\min(j) | a_{ij} > 0\} \end{cases} \quad (28)$$

and $\omega_{vt_i} \in \mathbb{R}^3$ represents the angular velocity of the virtual rigid body, and it is iteratively defined by

$$\begin{cases} \omega_{vt_i} = \lambda_{i0} \omega_0, \\ \omega_{vt_i} = (1 - \lambda_{ij}) \omega_j + \lambda_{ij} \omega_{vt_i}, \quad j = 1, \dots, n \end{cases} \quad (29)$$

Denote $\gamma_{ij} = \lambda_{ij} (1 - \lambda_{i(j+1)}) \dots (1 - \lambda_{in})$, then, the equation (29) can be rewritten as

$$\omega_{vt_i} = \sum_{j=0}^n \gamma_{ij} \omega_j, \quad (30)$$

where $\gamma_{ij} \in [0, 1]$, $i = 0, 1, \dots, n$ and $\sum_{j=0}^n \gamma_{ij} = 1$. The parameter $\gamma_{ij} > 0$ represents that UAV i could obtain information from UAV j , otherwise it is equal to zero. Similarly, the combination of the control torque τ_{vt_i} is given by

$$\tau_{vt_i} = \sum_{j=0}^n \gamma_{ij} \tau_j. \quad (31)$$

Based on the convexity in linear space, the translational dynamics of the virtual leader can be designed as follows

$$\begin{cases} \dot{p}_{vt_i} = v_{vt_i}, \\ \dot{v}_{vt_i} = g e_3 - \sum_{j=0}^n \gamma_{ij} ((f_j/m) R_j e_3), \end{cases} \quad (32)$$

where $p_{vt_i} = \sum_{j=0}^n \gamma_{ij} p_j$ and $v_{vt_i} = \sum_{j=0}^n \gamma_{ij} v_j$ represent the position and linear velocity of UAV i 's virtual leader.

The geometric convexity on $SO(3)$ can be viewed as the convex combination on the nonlinear manifold. In Euclidean space, connection of the line segments forms a convex hull. In nonlinear manifold, the connection of geodesics is named as geometric convexity on $SO(3)$, where the geodesics is the shortest path between two points on $SO(3)$. Let $B_r(I_3)$ be an open geodesic ball around the identity matrix in $SO(3)$ with the radius r . If $r < \pi/2$, the geodesics on $SO(3)$ is convex, and the geodesics on $SO(3)$ is weakly convex if $r < \pi$ [38]. In this paper, we define each rotation matrix satisfies $r < \pi$.

As seen from the form of the dynamics (26) and (32), they can be viewed as an under-actuated VTOL UAV perturbed by some disturbances. Since the communication topology has the hierarchical structure as shown in Fig. 3, the i -th virtual leader (26) (32) can be transformed into the dynamics (25) with subscript 0 once the state of its parent nodes converge to the leader's state. Thus, the following lemma is presented.

Lemma 5: Considering $n + 1$ under-actuated VTOL UAVs distributed in 3D space, if all UAVs have the same state after some moment, the dynamics of the virtual leader follows the form of (25).

Proof: Without loss of generality, we assume that $p_1 = p_2 = \dots = p_0$, $R_1 = R_2 = \dots = R_0$, and the corresponding velocities and control inputs are the same as the leader. Based on the fact that $\exp(\hat{\mathbf{0}}) = I_3$, $\log(I_3) = \hat{\mathbf{0}}$, $R_0 = \exp(\log(R_0))$, it leads to $R_{vt_i} = R_0$ by the iterative operation of (27). Since $\sum_{j=0}^n \gamma_{ij} = 1$, we have $\omega_{vt_i} = \omega_0$, $\tau_{vt_i} = \tau_0$, $p_{vt_i} = p_0$ and $v_{vt_i} = v_0$. Thus, the dynamics of UAV i 's virtual leader (26) and (32) have the form of equation (25) with the subscript 0. \square

For a networked system, the formation task in this paper is that the position p_i of each follower converges to $p_0 + d_{i0}$, the attitude R_i converges to $R_i^T R_d = I_3$ by the action of the control torque and force, where d_{i0} is some predefined constant which describes the formation shape. If $d_{i0} = \mathbf{0}$, based on Lemma 5, the consensus of the UAVs can be achieved. To accomplish the formation task, the consensus based formation tracking concept proposed in [18] can be adopted. Based on the two-stage trajectory tracking framework as seen in Section III and the proposed virtual leader structure, the formation tracking control law is summarized in Algorithm 1. The main results of formation tracking are presented in Theorem 2.

Theorem 2: Considering $n+1$ under-actuated VTOL UAVs being connected by a directed acyclic graph, and assuming that b_{1d}^i satisfy $b_{1d}^i \nparallel b_{3c}^i$, then the formation task can be achieved based on Algorithm 1, i.e.,

$$\lim_{t \rightarrow \infty} (p_i - p_0) = d_{i0}, \quad \lim_{t \rightarrow \infty} (v_i - v_0) = 0, \\ \lim_{t \rightarrow \infty} R_0^T R_i = I_3, \quad \lim_{t \rightarrow \infty} (\omega_i - \omega_0) = 0.$$

Proof: Since the dynamics (26) and (32) can be viewed as an under-actuated VTOL UAV perturbed by some known disturbances, UAV i is able to converge to its virtual leader based on the result of Theorem 1. As shown in Fig. 3, the hierarchical structure allows the UAVs in the first layer to

Algorithm 1 Formation Tracking of a Group of Under-Actuated VTOL UAVs

Step 1: For follower i , $i \in \{1, 2, \dots, n\}$, determine the set of its parent nodes $\mathcal{N}_i := \{j | a_{ij} > 0, j = 0, 1, \dots, n\}$.

Step 2: For follower i , construct its virtual leader vt_i according to (26) and (32).

Step 3: Design the virtual control input F_i as follows

$$F_i = k_1 \frac{e_p^i}{\sqrt{1 + e_p^{iT} e_p^i}} + k_2 \frac{e_v^i}{\sqrt{1 + e_v^{iT} e_v^i}} + \sum_{j=0}^n \gamma_{ij} \left(\frac{f_j}{m} R_j e_3 \right), \tag{33}$$

where $e_p^i = \tilde{p}_i - p_{vt_i}$, $e_v^i = v_i - v_{vt_i}$, $\tilde{p}_i = p_i - d_{i0}$, and $d_{i0} \in \mathbb{R}^3$ represents the desired relative position with respect to the leader.

Step 4: The thrust force f_i is given by

$$f_i = m \|F_i\|. \tag{34}$$

Step 5: Construct intermediary attitude R_c^i as follows

$$R_c^i = [b_{1c}^i, b_{2c}^i, b_{3c}^i] \in SO(3), \tag{35}$$

where

$$b_{3c}^i = \frac{F_i}{\|F_i\|}, b_{2c}^i = \frac{b_{3c}^i \times b_{1d}^i}{\|b_{3c}^i \times b_{1d}^i\|}, b_{1c}^i = b_{2c}^i \times b_{3c}^i$$

and $b_{1d}^i = R_{vt_i} e_1$.

Step 6: Determine the angular velocity ω_c^i and its accelerated velocity $\dot{\omega}_c^i$.

Step 7: Design the force control τ_i as follows:

$$\tau_i = -\alpha_1 e_E^i - \alpha_2 e_\omega^i - \sum_{j=0}^n \gamma_{ij} ((J \omega_j)^\wedge \omega_j) - J \dot{e}_\omega^i E_i^T \omega_c^i + J E_i^T \dot{\omega}_c^i, \tag{36}$$

where $E_i = R_{vt_i}^T R_i$, $e_E^i = [(E_i - E_i^T)^\vee] / [2(1 + \text{tr}(E_i))]$, and $e_\omega^i = \omega_i - E_i^T \omega_{vt_i}$.

achieve the formation task according to the trajectory tracking control approach presented in Theorem 1. Then, all the UAVs in the first layer satisfy the under-actuation constraints from the result of Lemma 5. After that, the UAVs in the second layer can perform the formation task successively. For other layers, the same stability can be achieved. Thus, the whole networked system can realize the formation task. \square

Remark 5: The set point stabilization for multiple under-actuated VTOL UAVs has wide applications, for example, multiple under-actuated VTOL UAVs landing, hovering-point standby and task switching. Based on the analysis of Section III – C, the Algorithm 1 can also achieve the set point formation stabilization for multiple UAVs.

V. NUMERICAL SIMULATIONS

In this section, the proposed coupled-attitude based formation theories are examined through numerical simulations.

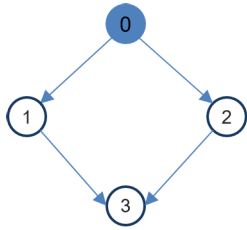


FIGURE 4. The communication graph for four vehicles.

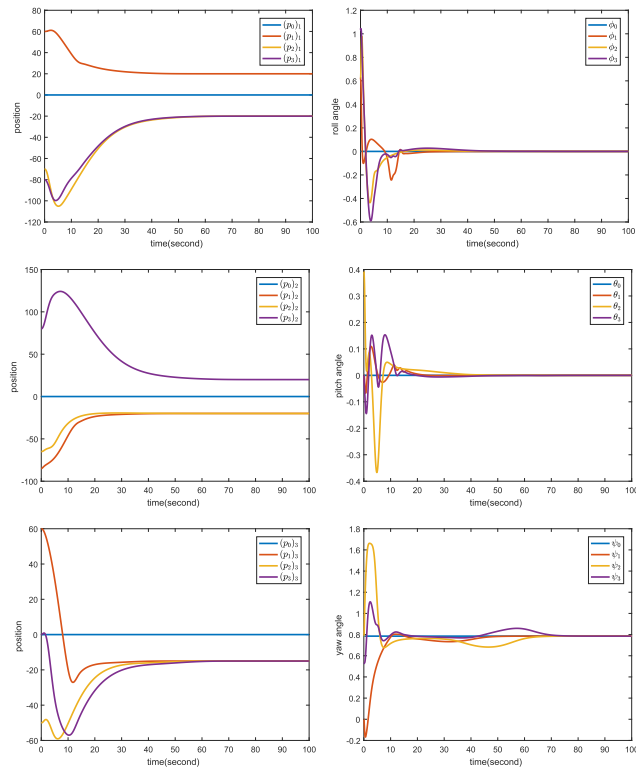


FIGURE 5. The evolutions of Euler-angles (ϕ_i, θ_i, ψ_i) and position p_i in the case of set points stabilization.

In the following part, two set of simulations are provided. The first is the set point stabilization for multiple UAVs and the second is to test the performance of formation tracking with a flying leader. Four under-actuated VTOL UAVs are involved in the simulations and one of them is the leader. The communication graph of the four UAVs is shown in Fig. 4. For each UAV, the mass $m = 4.34\text{kg}$, the inertia matrix $J = \text{diag}\{0.1, 0.2, 0.3\}\text{kg} \cdot \text{m}^2$, and the gravitational acceleration $g = 10\text{m} \cdot \text{s}^{-2}$.

A. SET POINT STABILIZATION FOR MULTIPLE UAVS

In this example, the set point stabilization for multiple UAVs is carried out. Based on Euler-angle, the rotation matrix $R_i = \exp(\psi_i \cdot \hat{e}_3) \exp(\theta_i \cdot \hat{e}_2) \exp(\phi_i \cdot \hat{e}_1)$. Let $\Theta_i = [\phi_i, \theta_i, \psi_i]^T$ be the set of Euler angles. The state of the leader are $p_0 = [0, 0, 0]^T$, and $\Theta_0 = [0, 0, \pi/4]^T$. The initial state of three followers are $p_1(0) = [60, -85, 60]^T$, $p_2(0) = [-70, -65, -50]^T$,

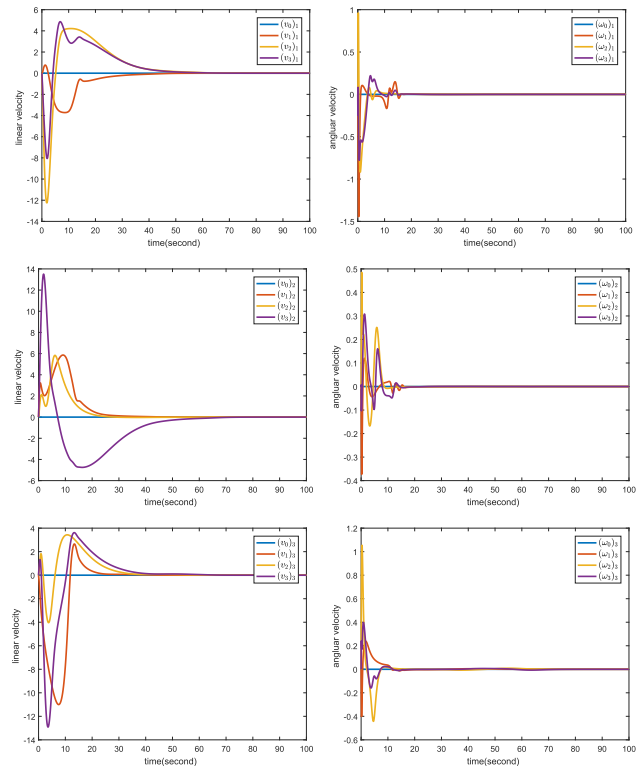


FIGURE 6. The evolutions of linear velocity v_i and angular velocity ω_i in the case of set points stabilization.

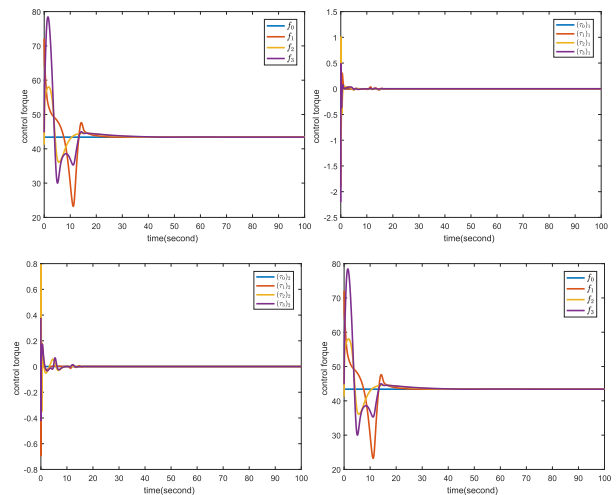


FIGURE 7. The control force f_i and torque τ_i in the case of set points stabilization.

$p_3(0) = [-80, 80, 0]^T$, $\Theta_1(0) = [\pi/5, 0, 0]^T$, $\Theta_2(0) = [\pi/5, \pi/8, \pi/4]^T$, $\Theta_3(0) = [\pi/3, 0, \pi/6]^T$, and $v_i(0) = \omega_i(0) = [0, 0, 0]^T, i = 1, 2, 3$. The gains of the controllers are chosen as $k_1 = 5, k_2 = 3, \alpha_1 = \alpha_2 = 0.5$, and the desired relative positions with respect to the leader are $d_{10} = [20, -20, -15]^T, d_{20} = [-20, -20, -15]^T, d_{30} = [-20, 20, -15]^T$. The evolutions of state are summarized in Fig. 5, Fig. 6, and Fig. 7. From these figures, we find that the task of set point stabilization for multiple under-actuated

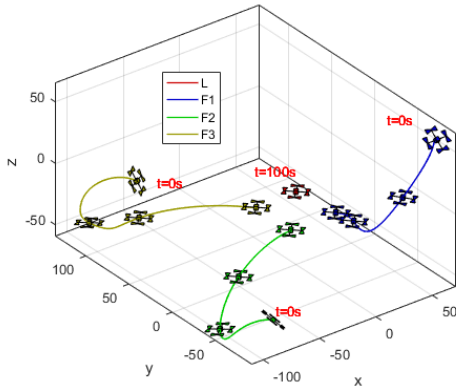


FIGURE 8. The evolutions of 3D space in the case of set points stabilization.

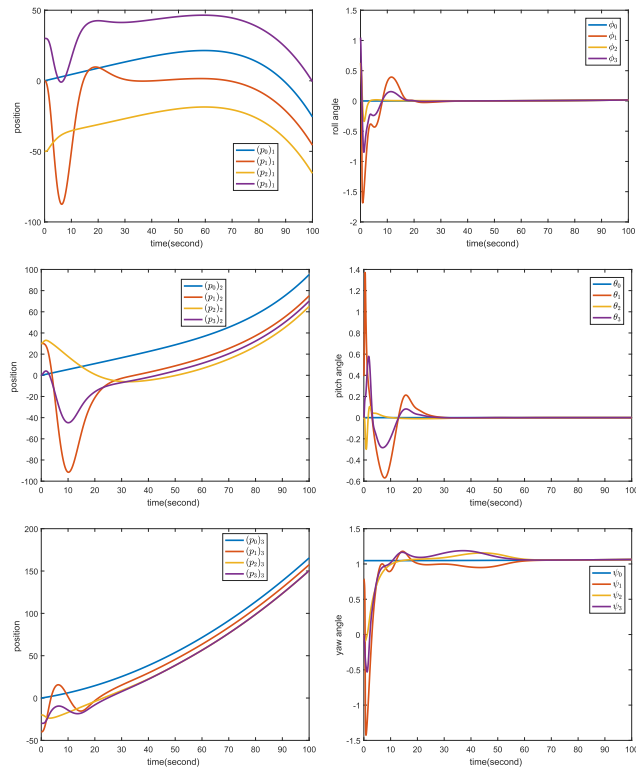


FIGURE 9. The evolutions of Euler-angles (ϕ_i, θ_i, ψ_i) and position p_i in the case of formation tracking.

VTOL UAVs is achieved. Moreover, the set point formation trajectories of the rigid bodies in 3D space are given Fig. 8. This simulation demonstrates that the proposed intermediate attitude can solve the state tracking problem.

B. FORMATION TRACKING FOR MULTIPLE UAVS

In this section, the formation tracking for multiple UAVs with a flying leader is examined. The initial state of the leader are $p_0(0) = \omega_0(0) = [0, 0, 0]^T$, $\Theta_0(0) = [0, 0, \pi/3]^T$ and $v_0(0) = [0.45, 0.55, 0.5]^T$. The control force and torque of the leader are $f_0 = 43.3\text{N}$ and $\tau_0 = [10^{-4} \sin(0.01t), 0, 10^{-4} \cos(0.01t)]^T \text{N}\cdot\text{m}$. The initial

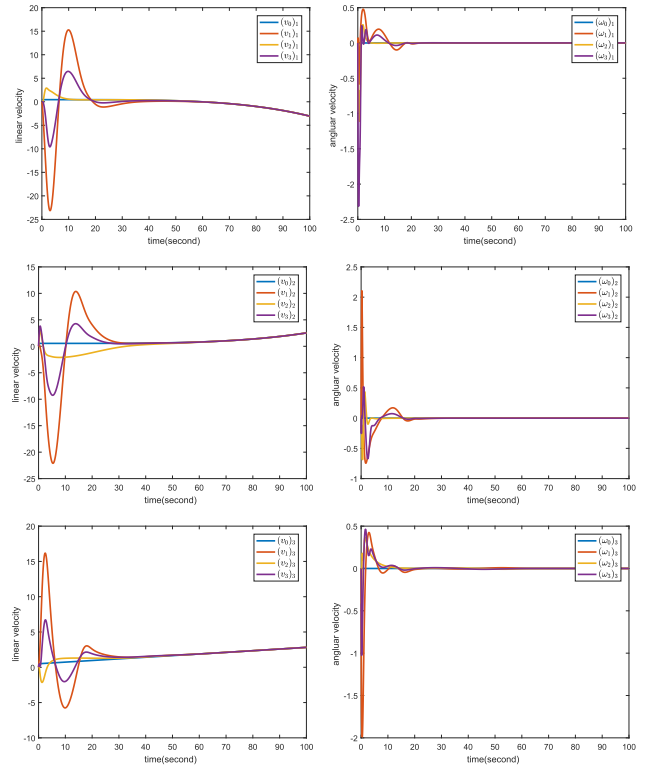


FIGURE 10. The evolutions of linear velocity v_i and angular velocity ω_i in the case of formation tracking.

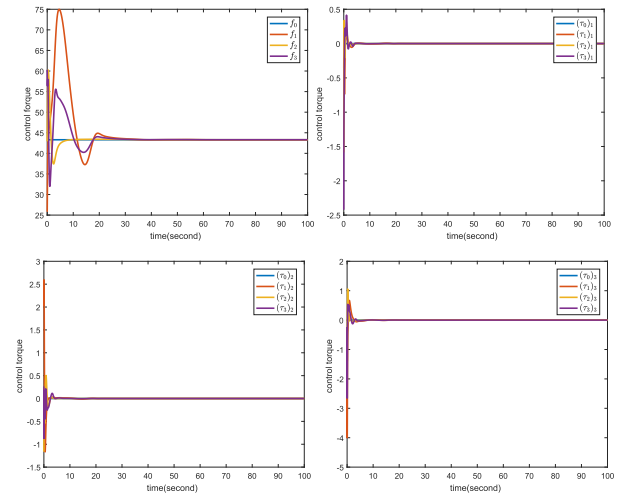


FIGURE 11. The control force f_i and torque τ_i in the case of formation tracking.

state of the three followers are $p_1(0) = [0, 30, -40]^T$, $p_2(0) = [-50, 30, -20]^T$, $p_3(0) = [-30, 0, -30]^T$, $\Theta_1(0) = [\pi/5, \pi/8, \pi/4]^T$, $\Theta_2(0) = [\pi/5, 0, 0]^T$, $\Theta_3(0) = [\pi/3, 0, 0]^T$, and $v_i(0) = \omega_i(0) = [0, 0, 0]^T$. The gains of the controllers are chosen to be the same as Section V-A, and the desired relative positions with respect to leader are $d_{10} = [-20, -20, -8]^T$, $d_{20} = [-40, -30, -15]^T$, $d_{30} = [25, -25, -15]^T$. The evolutions of the state are summarized in Fig. 9, Fig. 10, and Fig. 11, and these figures show that the

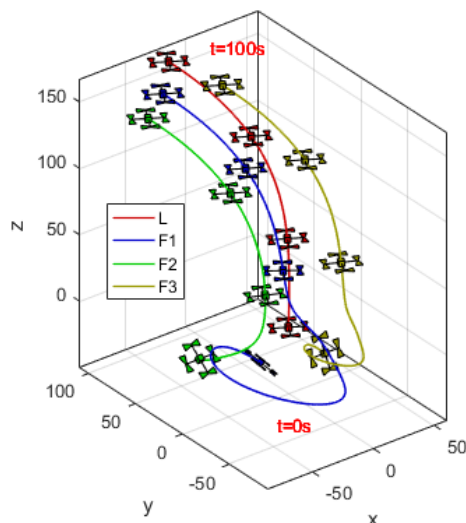


FIGURE 12. The evolutions of 3D space in the case of formation tracking.

formation tracking task for multiple under-actuated VTOL UAVs is realized. The 3D trajectories are given Fig. 12.

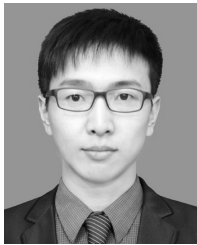
VI. CONCLUSION

In this paper, a full state tracking problem which includes both the position and attitude generated by an under-actuated VTOL UAV was studied. An intermediate attitude which can be seen as a bridge connecting the position and attitude motion was designed. Based on the intermediate attitude, we proposed a coupled-attitude based trajectory tracking scheme, and a simple formation tracking control under the directed acyclic graph. To the best of our knowledge, this is the first time that the concept of intermediate attitude was proposed based on which the appropriate controllers realizing the set point stabilization, trajectory tracking and formation tracking were designed, where the trajectory of the leader is generated by a real vehicle which has the same dynamics as the followers. Simulation results were provided to validate the performance of the proposed control approach.

REFERENCES

- [1] Z. Qu, *Cooperative Control of Dynamical Systems: Applications to Autonomous Vehicles*. New York, NY, USA: Springer-Verlag, 2009.
- [2] W. Ren and Y. Cao, *Distributed Coordination of Multi-Agent Networks: Emergent Problems, Models, and Issues*. London, U.K.: Springer-Verlag, 2011.
- [3] X. Dong, B. Yu, Z. Shi, and Y. Zhong, "Time-varying formation control for unmanned aerial vehicles: Theories and applications," *IEEE Trans. Control Syst. Technol.*, vol. 23, no. 1, pp. 340–348, Jan. 2015.
- [4] Y. Zhao, Z. Duan, G. Wen, and Y. Zhang, "Distributed finite-time tracking control for multi-agent systems: An observer-based approach," *Syst. Control Lett.*, vol. 62, no. 1, pp. 22–28, 2013.
- [5] R. Li and G.-H. Yang, "Consensus control of a class of uncertain nonlinear multiagent systems via gradient-based algorithms," *IEEE Trans. Cybern.*, Apr. 2018, doi: 10.1109/TCYB.2018.2819361.
- [6] J. A. Fax and R. M. Murray, "Information flow and cooperative control of vehicle formations," *IEEE Trans. Autom. Control*, vol. 49, no. 9, pp. 1465–1476, Sep. 2004.
- [7] Y. Cao, D. Stuart, W. Ren, and Z. Meng, "Distributed containment control for multiple autonomous vehicles with double-integrator dynamics: Algorithms and experiments," *IEEE Trans. Control Syst. Technol.*, vol. 19, no. 4, pp. 929–938, Jul. 2011.
- [8] Z. Li, Z. Duan, G. Chen, and L. Huang, "Consensus of multiagent systems and synchronization of complex networks: A unified viewpoint," *IEEE Trans. Circuits Syst. I, Reg. Papers*, vol. 57, no. 1, pp. 213–224, Jan. 2010.
- [9] Y. Zhao, Y. Liu, G. Wen, X. Yu, and G. Chen, "Distributed average tracking for Lipschitz-type of nonlinear dynamical systems," *IEEE Trans. Cybern.*, Aug. 2018, doi: 10.1109/TCYB.2018.2859352.
- [10] Q. Wang and J. Wang, "Fully distributed fault-tolerant consensus protocols for Lipschitz nonlinear multi-agent systems," *IEEE Access*, vol. 6, pp. 17313–17325, 2018.
- [11] H. Cai and J. Huang, "The leader-following consensus for multiple uncertain Euler-lagrange systems with an adaptive distributed observer," *IEEE Trans. Autom. Control*, vol. 61, no. 10, pp. 3152–3157, Oct. 2016.
- [12] N. Huang, Z. Duan, G. Wen, and Y. Zhao, "Event-triggered consensus tracking of multi-agent systems with Lur'e nonlinear dynamics," *Int. J. Control*, vol. 89, no. 5, pp. 1025–1037, 2016.
- [13] F. Bullo and A. D. Lewis, *Geometric Control of Mechanical Systems*. New York, NY, USA: Springer, 2005.
- [14] Y. Xia, Z. Zhu, M. Fu, and S. Wang, "Attitude tracking of rigid spacecraft with bounded disturbances," *IEEE Trans. Ind. Electron.*, vol. 58, no. 2, pp. 647–659, Feb. 2011.
- [15] A. Sarlette, R. Sepulchre, and N. E. Leonard, "Autonomous rigid body attitude synchronization," *Automatica*, vol. 45, no. 2, pp. 572–577, Feb. 2009.
- [16] J. Thunberg, J. Goncalves, and X. Hu, "Consensus and formation control on SE(3) for switching topologies," *Automatica*, vol. 66, pp. 109–121, Apr. 2016.
- [17] A.-M. Zou, K. D. Kumar, and Z.-G. Hou, "Attitude coordination control for a group of spacecraft without velocity measurements," *IEEE Trans. Control Syst. Technol.*, vol. 20, no. 5, pp. 1160–1174, Sep. 2012.
- [18] R. Dong and Z. Geng, "Consensus for formation control of multi-agent systems," *Int. J. Robust Nonlinear Control*, vol. 25, no. 14, pp. 2481–2501, Aug. 2015.
- [19] Y. Liu, Y. Zhao, and G. Chen, "Finite-time formation tracking control for multiple vehicles: A motion planning approach," *Int. J. Robust Nonlinear Control*, vol. 26, no. 14, pp. 3130–3149, Sep. 2016.
- [20] Z. Xue, J. Wang, Q. Shi, G. Ding, and Q. Wu, "Time-frequency scheduling and power optimization for reliable multiple UAV communications," *IEEE Access*, vol. 6, pp. 3992–4005, Jan. 2018, doi: 10.1109/ACCESS.2018.2790933.
- [21] H. Li, W. Yan, and Y. Shi, "Continuous-time model predictive control of under-actuated spacecraft with bounded control torques," *Automatica*, vol. 75, pp. 144–153, Jan. 2017.
- [22] A. Isidori, *Nonlinear Control Systems*, 3rd ed. New York, NY, USA: Springer, 1995.
- [23] A. Abdessameud and A. Tayebi, "Global trajectory tracking control of VTOL-UAVs without linear velocity measurements," *Automatica*, vol. 46, pp. 1053–1059, Jun. 2010.
- [24] A. Roberts and A. Tayebi, "Adaptive position tracking of VTOL UAVs," *IEEE Trans. Robot.*, vol. 27, no. 1, pp. 129–142, Feb. 2011.
- [25] H. Du, W. Zhu, G. Wen, Z. Duan, and J. Lü, "Distributed formation control of multiple quadrotor aircraft based on nonsmooth consensus algorithms," *IEEE Trans. Cybern.*, vol. 49, no. 1, pp. 342–353, Jan. 2019, doi: 10.1109/TCYB.2017.2777463.
- [26] T. Lee, M. Leok, and N. McClamroch, "Geometric tracking control of a quadrotor UAV on SE(3)," in *Proc. 49th IEEE Conf. Decis. Control (CDC)*, Dec. 2010, pp. 5420–5425.
- [27] Y. Yu and X. Ding, "A global tracking controller for underactuated aerial vehicles: Design, analysis, and experimental tests on quadrotor," *IEEE/ASME Trans. Mechatronics*, vol. 21, no. 5, pp. 2499–2511, Oct. 2016.
- [28] Y. Zou and Z. Meng, "Immersion and invariance-based adaptive controller for quadrotor systems," *IEEE Trans. Syst., Man, Cybern., Syst.*, Jan. 2018, doi: 10.1109/TSMC.2018.2790929.
- [29] Y. Zou, "Trajectory tracking controller for quadrotors without velocity and angular velocity measurements," *IET Control Theory Appl.*, vol. 11, no. 1, pp. 101–109, Jan. 2017.
- [30] H. Wang, "Second-order consensus of networked thrust-propelled vehicles on directed graphs," *IEEE Trans. Autom. Control*, vol. 61, no. 1, pp. 222–227, Jan. 2016.
- [31] Y. Zou, Z. Zhou, X. Dong, and Z. Meng, "Distributed formation control for multiple vertical takeoff and landing UAVs with switching topologies," *IEEE/ASME Trans. Mechatronics*, vol. 23, no. 4, pp. 1750–1761, Aug. 2018.

- [32] A. Loria and E. Panteley, *Advanced Topics in Control Systems Theory: Lecture Notes from FAP 2004*. New York, NY, USA: Springer-Verlag, 2005.
- [33] W. Ding, G. Yan, and Z. Lin, "Collective motions and formations under pursuit strategies on directed acyclic graphs," *Automatica*, vol. 46, no. 1, pp. 174–181, Jan. 2010.
- [34] D. E. Zlotnik and J. R. Forbes, "Exponential convergence of a nonlinear attitude estimator," *Automatica*, vol. 72, pp. 11–18, Oct. 2016.
- [35] Z.-P. Jiang, E. Lefeber, and H. Nijmeijer, "Saturated stabilization and tracking of a nonholonomic mobile robot," *Syst. Control Lett.*, vol. 42, no. 5, pp. 327–332, Apr. 2001.
- [36] T. Liu and Z.-P. Jiang, "Distributed formation control of nonholonomic mobile robots without global position measurements," *Automatica*, vol. 49, no. 2, pp. 592–600, Feb. 2013.
- [37] X. Peng, J. Sun, and Z. Geng, "The geometric convexity on SE(3) and its application to the formation tracking in multi-vehicle systems," *Int. J. Control*, Aug. 2017, doi: [10.1080/00207179.2017.1361043](https://doi.org/10.1080/00207179.2017.1361043).
- [38] R. Hartley, J. Trumpf, Y. Dai, and H. Li, "Rotation averaging," *Int. J. Comput. Vis.*, vol. 103, no. 3, pp. 267–305, Jul. 2013.



XIUHUI PENG was born in Dezhou, China. He received the B.S. degree in automatic control from Jiangnan University, Wuxi, China, in 2014. He is currently pursuing the Ph.D. degree in mechanics and engineering science with the School of Engineering, Peking University.

His research interests include cooperative control, unmanned systems control, and nonlinear control of mechanical systems.



KEXIN GUO received the B.S. degree in control theory and control engineering from the Beijing Institute of Technology, Beijing, China, in 2011, the M.S. degree in instrumentation science and technology from the Beijing University of Aeronautics and Astronautics, Beijing, in 2014, and the Ph.D. degree from the School of Electrical and Electronic Engineering, Nanyang Technological University, Singapore, in 2018.

His research interests include GPS-denied localization, formation control, and unmanned systems.



ZHIYONG GENG received the B.S. and M.S. degrees in engineering from Northeastern University, Shenyang, China, in 1981 and 1984, respectively, and the Ph.D. degree from the Institute of Systems Science, Chinese Academy of Sciences, in 1995. He was a Postdoctoral Research Fellow with the Department of Mechanics and Engineering Science, Peking University, from 1995 to 1997, where he is currently a Professor with the State Key Laboratory for Turbulence and Complex Systems and the Department of Mechanics and Engineering Science.

His research interests include robust control and nonlinear control.

• • •